Journal of Geography, Regional Planning and Development
Homepage : https://journal.antispublisher.id/index.php/JGRPD
Email : admin@antispublisher.com

e-ISSN : 3032-131X
JGRPD, Vol. 2, No. 3, March 2025
Page 132-147


# The Impact of Desertification on Agricultural Lands in Laylan Sub-district through the Application of Artificial Intelligence

**Manal Saahi Mohammed Darwish**
Samarra University, Iraq



**DOI : https://doi.org/10.61796/jgrpd.v2i3.1452**

**Sections Info**

***Article history:***
Submitted: February 05, 2025
Final Revised: February 13, 2025
Accepted: March 07, 2025
Published: March 30, 2025

***Keywords:***
Land degradation
Desertification Risk Index (DRI)
Normalized Multi-band Drought Index (NMDI)
Soil Salinity Index (SI)
Remote sensing
ArcGIS
Lailan subdistrict
Sustainable land management

**ABSTRACT**

***Objective:*** *This study aims to assess land degradation and desertification risk in Lailan Subdistrict by integrating remote sensing indices to identify environmental stressors affecting agricultural productivity.* ***Method:*** *Landsat OLI 8 satellite imagery and ArcGIS 10.4.1 were employed to analyze three key indicators: the Desertification Risk Index (DRI), Normalized Multi-band Drought Index (NMDI), and Soil Salinity Index (SI).* ***Results:*** *The total study area of 694.84 km² was classified into five desertification risk levels, ranging from low (6.51%) to extreme (10.15%). Moderate and severe drought collectively affected over 57% of the area, with extreme drought alone covering 39.14%. Soil salinity varied widely, with moderate (31.20%) and high salinity (27.45%) dominating the landscape, while very high salinity (>30 dS/m) affected 8.65% of the area. Overall, more than 70% of the subdistrict was exposed to critical risks driven by combined drought stress, salinization, and unsustainable land use.* ***Novelty:*** *By integrating multiple remote sensing indices, this research provides a comprehensive spatial assessment of desertification risks, offering practical insights for sustainable land management strategies, including improved irrigation, salt-tolerant crops, vegetation restoration, and long-term monitoring.*

## INTRODUCTION

Desertification is one of the most pressing global environmental challenges, particularly in arid and semi-arid regions characterized by fragile ecosystems and vulnerable to both climatic fluctuations and unsustainable human practices. The problem has been exacerbated by overgrazing, improper agricultural techniques, population pressure, and irrational exploitation of natural resources, in addition to pollution and climate change. Iraq is among the countries severely affected by desertification, where agricultural lands have increasingly deteriorated in both productivity and area, especially after 2003 due to socio-economic disruptions, water scarcity, energy shortages, and urban expansion. These factors have contributed to soil degradation, salinization, and the transformation of large areas of farmland into desertified or non-agricultural land, posing a serious threat to agricultural sustainability and food security [1], [2], [3].

### Research Problem

Desertification is one of the most complex environmental issues, with both natural and human dimensions, leaving widespread negative impacts on social and economic systems, particularly on agricultural activities. Accordingly, the research problem revolves around the following questions:

1. What is the reality of desertification in the Al-Nasaf district? What are its main driving factors? Can it primarily be attributed to natural causes, human activities, or the interaction between the two?
2. In what forms does desertification manifest in the study area, and to what extent does it affect agricultural activities?
3. What measures and procedures can be adopted to mitigate desertification? Is it possible to rehabilitate degraded lands and restore their agricultural productivity?

**Research Hypotheses**

A. The study assumes that both natural and human factors jointly contribute significantly to the emergence of desertification, with human activities in particular playing a key role in aggravating the problem through their interaction with natural conditions.
B. It is further hypothesized that desertification negatively affects agricultural activities in the study area, leading to a reduction in cultivable land and a decline in crop productivity.

**Research Significance**

1. Highlighting the severity of desertification on agricultural lands in Laylan sub-district and its resulting socio-economic impacts.
2.Employing Artificial Intelligence (AI) techniques—such as machine learning and satellite image processing—for precise detection of changes in vegetation cover and soil conditions.
3.Providing high-resolution quantitative and spatial data to assist decision-makers and agricultural planners in designing effective strategies to combat desertification.
4.Contributing to the sustainability of agricultural resources by proposing scientific and technological solutions that enhance land management efficiency.
5.Enriching environmental geographical studies through the integration of spatial analysis and AI as an emerging research direction.

**Research Objectives**

1. Analyze the extent of desertification in Laylan sub-district and identify the natural and human factors driving it.
2.Apply AI techniques (e.g., machine learning algorithms and neural networks) to detect changes in vegetation cover and soil properties using satellite imagery and field data.
3. Accurately estimate the spatial and temporal extent of agricultural lands affected by desertification.
4.Assess the impact of desertification on agricultural production and crop yields in Laylan sub-district.
5.Provide AI-driven recommendations and solutions to mitigate desertification and promote agricultural land sustainability.

**Study Area Boundaries**

The study area is geographically located between longitudes (′19°44– ′48°44E) and latitudes (′15°35– ′31°35N), as shown in Map (1), covering an area of 671.5km². Administratively, it belongs to Kirkuk Governorate. It is bounded to the north and northwest by the Jambur Plateau, to the east by the Qader Karam region, to the south by

the Jambur Hills and Taza sub-district, and to the west by the boundaries of Kirkuk city center, as illustrated in the study area map [4].

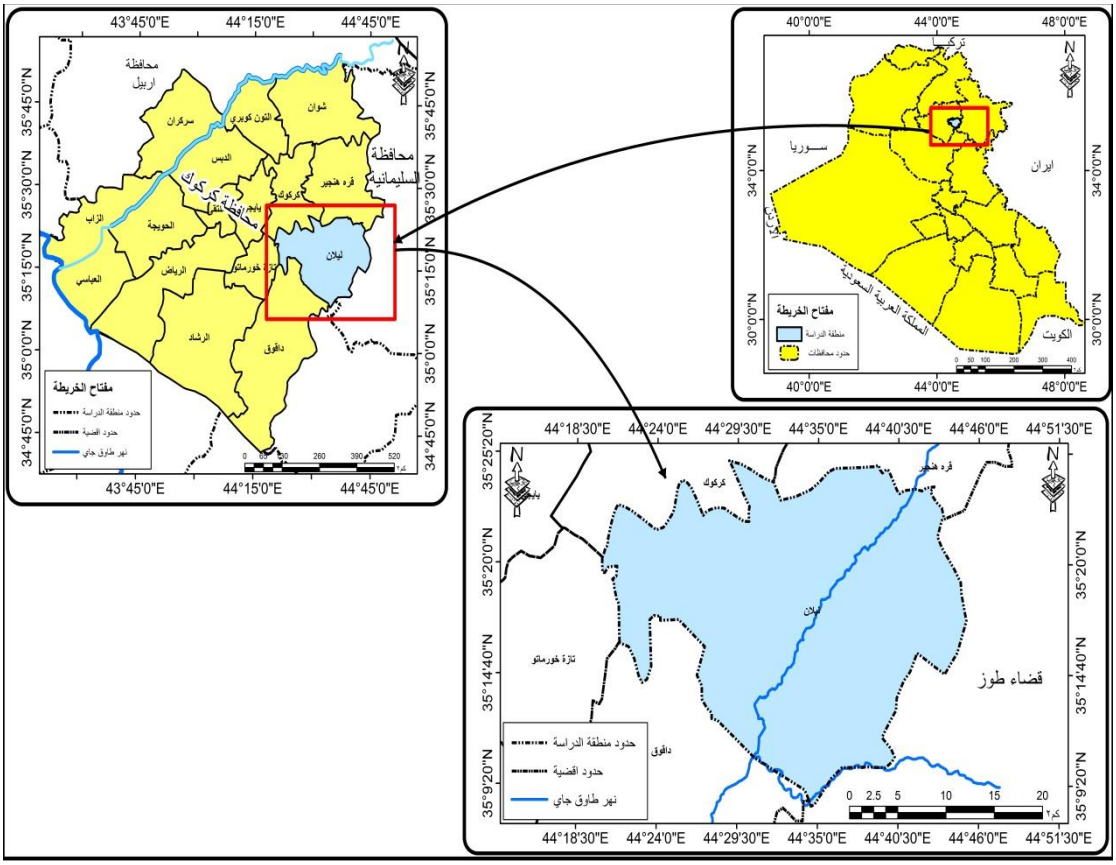


**Map 1.** The location of the study area.

Source: Prepared by the researcher based on the Ministry of Water Resources, General Commission for Survey, Administrative Map of Iraq at a scale of 1:1,000,000(2023), using ArcGIS .10.4.1.

## RESEARCH METHOD

The study adopted the descriptive–analytical approach to examine the impact of desertification on agricultural lands in Laylan Subdistrict, relying on both field and remote sensing data. Landsat satellite imagery for the period 2005–2024 was processed and corrected, in addition to climatic data (precipitation, temperature, humidity) and official agricultural statistics.

Geographic Information Systems (GIS) and remote sensing techniques were employed to extract environmental indicators such as the Normalized Difference Vegetation Index (NDVI) as well as drought and salinity indices

## RESULTS AND DISCUSSION

### *Results*

### Axis Two:

### Normalized Difference Vegetation Index (NDVI)

This index is used in land degradation studies as an indicator of vegetation density. It relies on the differential interaction of chlorophyll within plants with electromagnetic radiation. NDVI is widely applied in drought monitoring, agricultural productivity assessment and prediction, and in forecasting areas prone to fire hazards [5].

To calculate NDVI, remote sensing data must include a band covering the red. region of the electromagnetic spectrum and another covering the near-infrared (NIR) region. Most vegetation indices involve more than one spectral band, but are limited to specific spectral ranges in the visible and near-infrared spectrum, as these bands capture nearly %90of vegetation-related information [6], [7].

NDVI represents the difference between the near-infrared band (0.85– 0.88µm) and the red band (0.64– 0.67µm), divided by their sum, producing values ranging between – 1and +1. Positive values close to + 1indicate dense vegetation (appearing in light white tones), while values near– 1indicate non-vegetated surface features. The NDVI is calculated using the following formula [8], [9]:

NDVI = (NIR.BAND 5- RED.BAND4)}{(NIR.BAND 5+ RED.BAND4) (Landsat 8 OLI) . Based on Map (2), Table (1), and Figure (1), the NDVI values in the study area for the year 2024were classified into four categories:

Dense Vegetation Cover: This class includes lands with dense vegetation, covering an area of 17.93km² (%2.58) of the total area. It is mostly concentrated near water sources.

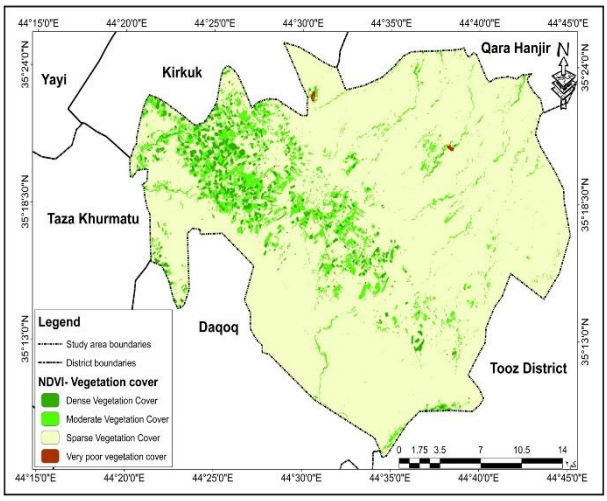


**Map 2.** NDVI classes for the study area in 2024

Source: Prepared by the researcher based on Landsat 8 OLI imagery, processed using ArcMap 10.4.1, dated 25/9/2024.

**Table 1.** Area and percentage of vegetation cover in the study area, 2024.

| Class | Area (km²) | Percentage (%) |
|---|---|---|
| Dense Vegetation | 17.93 | 2.58 |
| Moderate Vegetation | 60.32 | 8.68 |
| Sparse Vegetation | 615.81 | 88.63 |
| Very Sparse Vegetation | 0.78 | 0.11 |
| Total | 694.84 | 100% |

Source: Prepared by the researcher based on Map 2.

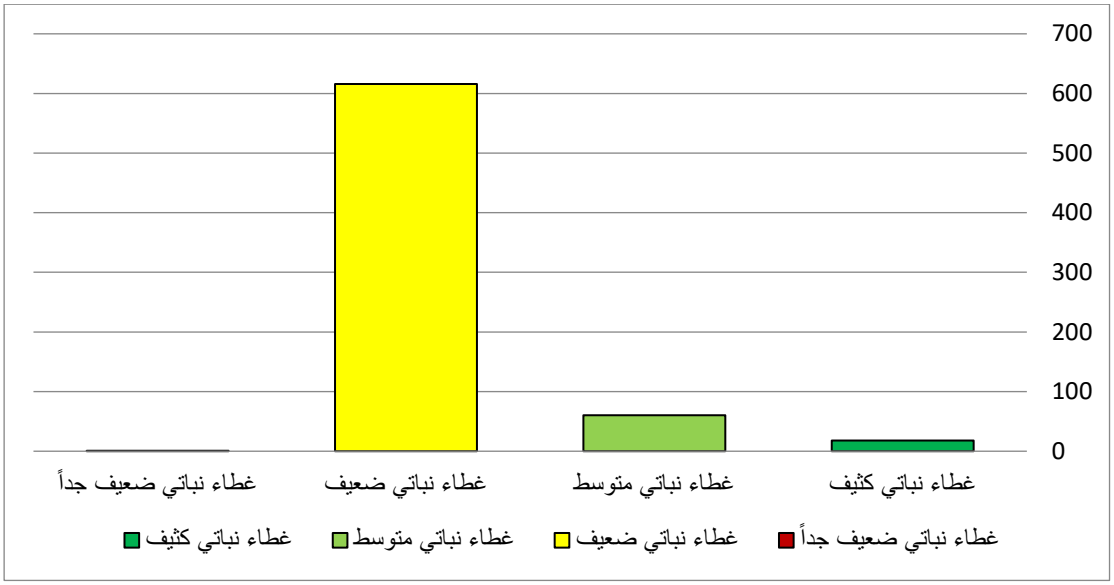


**Figure 1.** Area and percentage of vegetation cover in the study area, 2024.
Source: Prepared by the researcher based on Table 1.

Moderate Vegetation Cover: Lands with moderate vegetation density, covering 60.32 km² (8.68%) of the total area.

Sparse Vegetation Cover: Areas with scattered or rarely existing vegetation, covering 615.81 km² (88.63%) of the total area.

Very Sparse Vegetation Cover: Includes water-covered areas, with an extent of 0.78 km² (0.11%) of the total area.

**Land Degradation Index (LDI)**

This index is considered one of the key tools for detecting degradation risks by measuring the degree of soil deterioration. Such degradation is typically manifested in the gradual decline of soil fertility, which consequently leads to a reduction in crop productivity. Undoubtedly, prevailing climatic factors play a crucial role in this phenomenon, particularly since the study area falls within arid and semi-arid regions. The decline in soil fertility results in the shrinkage of vegetation cover and the expansion of barren soils, thereby increasing the likelihood of soil exposure to erosion processes caused by both water and wind.

As illustrated in Map (3) and Table (2), the lands exposed to degradation and the method of identifying degradation risks are clearly demonstrated. According to this index, the study area was classified into five categories as follows:

$$LDI = 1 \div ((255 - BAND.BLUE2 + BAND.GREEN3) \div ((255 + (BAND.BLUE2 + BAND.GREEN3))$$

**Non-degraded lands:**

This category is distributed along the riverbank soils, as shown in Table (1). The total area of this class reached 18.91km², representing %2.72 of the total area of the study region.

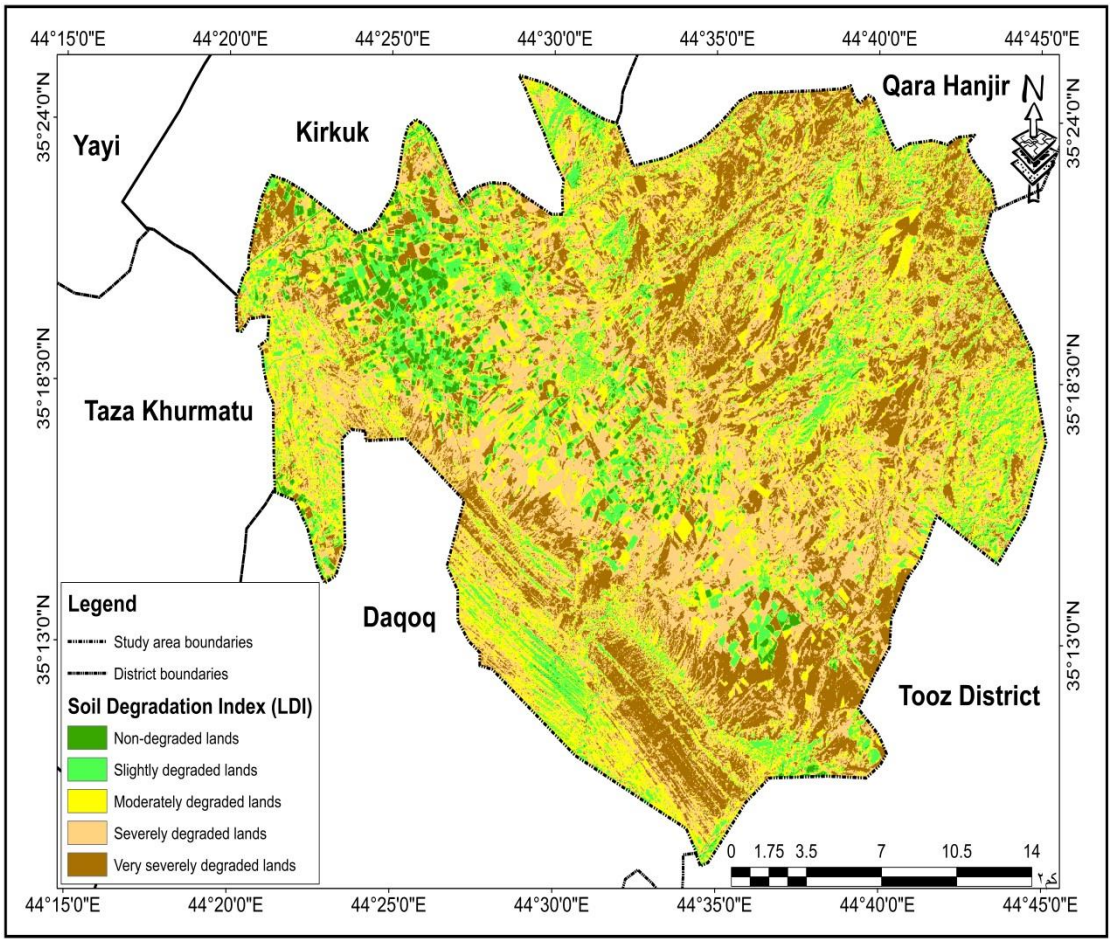


**Map 3.** Land Degradation Index (LDI) for the Study Area 2024

Source: Prepared by the researcher based on satellite imagery (Landsat 8OLI) and outputs from ArcMap 10.4.1, dated .2024/09/25

**Table 2.** Area (km²) according to the Land Degradation Index (LDI) for the year .2024

| Percentage (%) | Area (km²) | Salinity index) LDI( |
|---|---|---|
| 2.72% | 18.91 | Non-degraded lands |
| 12.44% | 86.42 | Slightly degraded lands |
| 25.84% | 179.53 | Moderately degraded lands |
| 35.02% | 243.33 | Severely degraded lands |
| 23.98% | 166.65 | Very severely degraded lands |
| 100% | 694.84 | Total |

Source: Prepared by the researcher based on map 3.

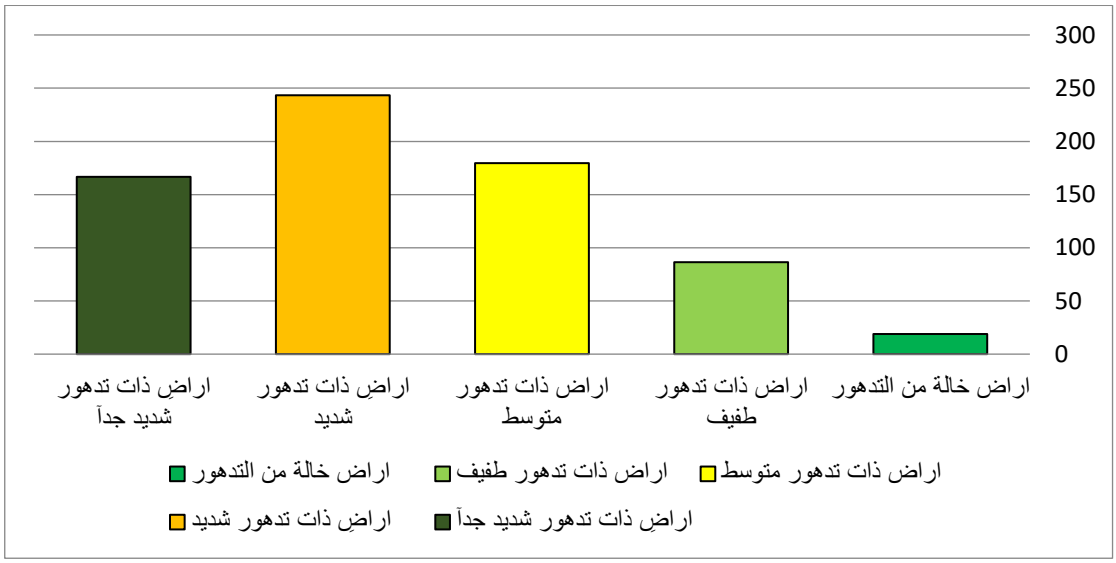


**Figure 2.** Area (km²) according to the Land Degradation Index (LDI) for the year .2024
Source: Prepared by the researcher based on the data from Table (3).

Slightly Degraded Lands: This category is concentrated in some riverbank soils and their alluvial clay basins. As shown in Table (2), this class covers an area of 86.42 km², representing 12.44% of the total study area.

Moderately Degraded Lands: This level appears in scattered locations within clay-filled river basins, particularly in soils of poor quality. According to Table (2), the area of this class reached 179.53 km², equivalent to 25.84% of the total area.

Highly Degraded Lands: This level is represented by dry soils in some clay-filled river basins with poor-quality soils, as well as sandy dune soils. As indicated in Table (2), this class covers 243.33 km², accounting for 35.02% of the total area.

Very Highly Degraded Lands: These lands are found in dry areas lacking vegetation cover and exposed to wind and water erosion. Table (2) shows that this class occupies 166.65 km², representing 23.98% of the total area.

**Normalized Multi-band Drought Index (NMDI):**

This index considers soil moisture background to monitor potential drought conditions. Three specific ranges were selected due to their unique response to changes in soil moisture and vegetation cover. The index uses the difference in water absorption in the shortwave infrared region (1640 and 2130 nm) as a measure of water sensitivity in vegetation and soil. It is also commonly used for forest fire detection.

As soil moisture increases, the index values decrease. The index ranges are: 0.7 to 1 for dry soils, 0.6 to 0.7 for moderately moist soils, less than 0.6 for wet soils.

1. Non-Drought Lands: This class is concentrated in riverbank soils and soils with very high moisture and dense vegetation, especially in the northwestern parts of the study area. Based on Map (4), Table (3), and Figure (3), this class ranks fourth with an area of 12.9 km², representing 1.86% of the total study area.
2. Slightly Drought-Affected Lands: This level occurs in some riverbank soils and alluvial clay basins, characterized by high moisture and dense vegetation,

particularly in the central and southern parts of the study area. According to Table (3) and Map (3), this class covers 12.51 km², equivalent to 1.80% of the total area.

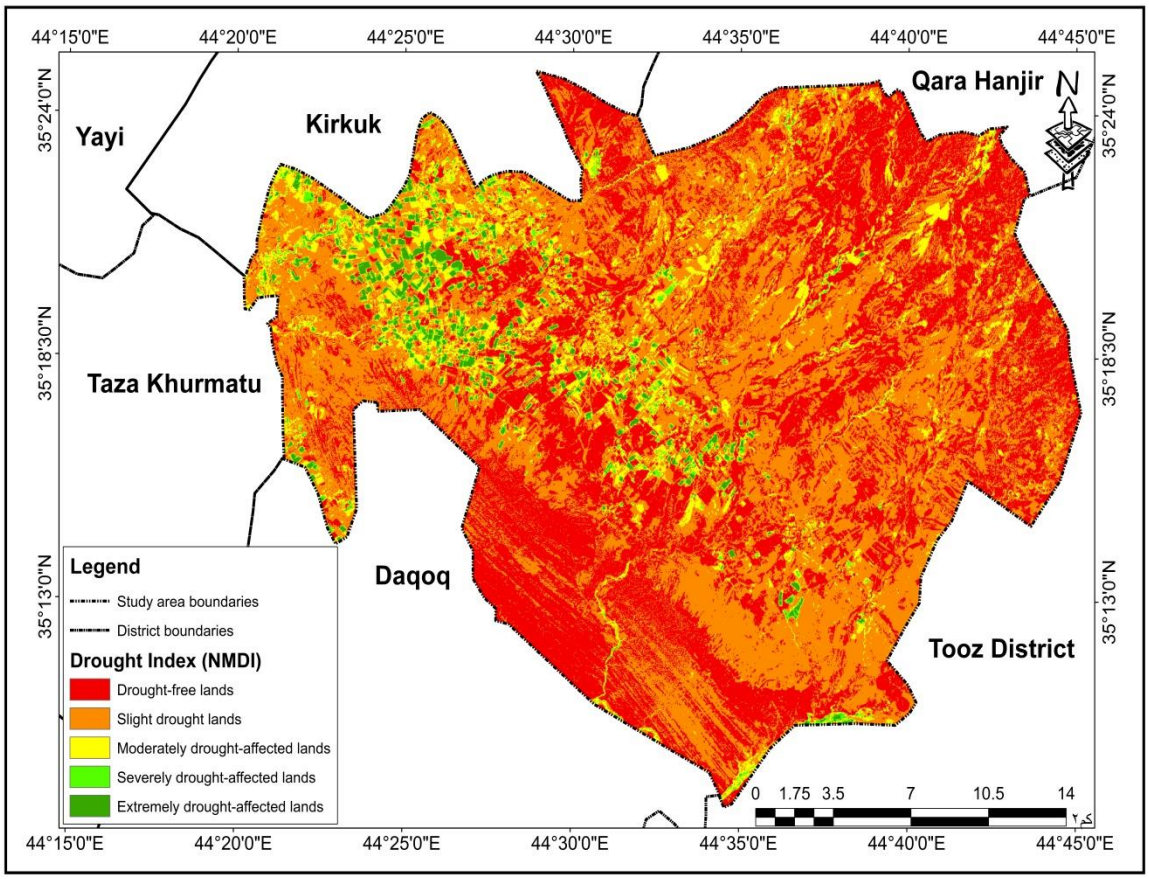


**Map 4.** Normalized Multi-band Drought Index (NMDI) for the study area.
Source: Prepared by the researcher based on satellite imagery from the American satellite (Landsat OLI 8) dated 25/09/2024, using ArcGIS 10.4.1.

Table 3. Areas according to the Normalized Multi-band Drought Index (NMDI) for the study area.

| Percentage (%) | Area (km²) | Drought Classes | T |
|---|---|---|---|
| 39.14 | 271.96 | Extremely drought-affected lands | 1 |
| 48.84 | 339.34 | Severely drought-affected lands | 2 |
| 8.37 | 58.13 | Moderately drought-affected lands | 3 |
| 1.80 | 12.51 | Slight drought lands | 4 |
| 1.86 | 12.9 | Drought-free lands | 5 |
| 100% | 694.84 | Total | |

Source: Prepared by the researcher based on Figure (4).

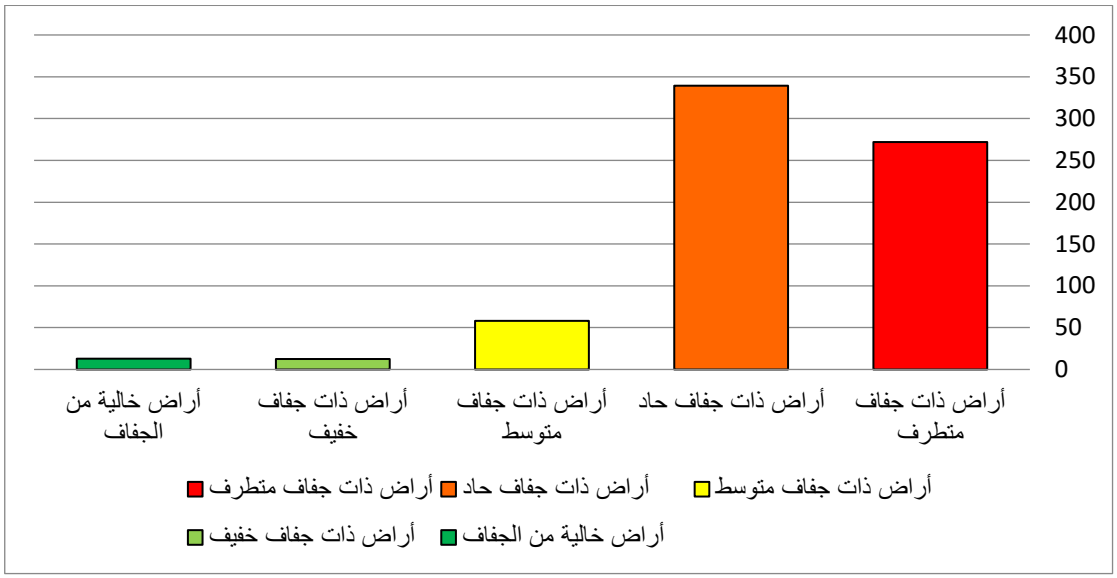


**Figure 3.** Areas according to the Normalized Multi-band Drought Index (NMDI) for the study area.

Source: Prepared by the researcher based on Table (5).

Moderately Drought-Affected Lands: This class occurs in scattered locations within clay-filled river basins, particularly in poor-quality soils, characterized by medium soil moisture and vegetation density. Based on Table (3) and Figure (3), the area of this class reached 58.13 km², representing 8.37% of the total area.

Severely Drought-Affected Lands: This level is concentrated in dry soils of some clay-filled river basins and sandy dune soils. According to Table (3) and Figure (3), this class covers 339.34 km², accounting for 48.84% of the total study area.

Extremely Drought-Affected Lands: These lands are found in dry areas lacking vegetation cover. Table (3) and Figure (3) indicate that this class occupies 271.96 km², equivalent to 39.14% of the study area.

Variations in drought levels are associated with several climatic and natural factors, most notably increased solar incidence angle, longer daylight hours, and higher incoming radiation exceeding outgoing radiation, which leads to significant heat accumulation coinciding with reduced soil moisture during the hot season. Additionally, the presence of Lake Tharthar as an important water source helps mitigate drought severity, particularly in agricultural lands along riverbanks, where drought appears slight or nearly absent in upstream areas. Moreover, lower soil moisture during the hot season increases evaporation rates and water consumption by crops, reducing relative humidity. High drought values further enhance evaporation, contributing to soil salinization through surface water evaporation or upward capillary movement of saline groundwater.

**Soil Salinity Index (SI):**

Salinity is one of the main phenomena associated with desertification and a key limiting factor for agricultural production, potentially rendering soils unfit for cultivation. Accumulation of soluble salts and conversion of soils into saline and saline-

alkaline types cause severe problems for plant growth. The issue of salinity dates back to before 2400 BCE, linked directly to irrigation practices that led to soil degradation, depletion, and ecological changes. Salinity can destroy agricultural and rangeland areas, transforming them into unproductive desertified lands.

Globally, salinity affects approximately 950 million hectares, with some estimates indicating a loss of three hectares of agricultural land per minute due to salinization. The 2008 Global Desertification Map showed that about 8 million km² are at risk of salinity without proper mitigation measures. In Iraq, roughly 8.5 million hectares (34 million donums out of 11.5 million hectares, or 46 million donums, of arable land) are affected by salinity, representing 74% of total arable land.

Based on the Soil Salinity Index (SI) for Lailan Subdistrict, a quantitative representation using area and color was applied to highlight spatial and temporal variations of affected lands. The analysis relied on satellite imagery, revealing significant changes in salinity due to natural factors and human activities. Salinized lands in Lailan were classified into five categories, as shown in Map (5).

**Very Low Salinity Lands:**

This class represents soils with salinity below 4 dS/m, found in some riverbank soils, sandy dunes, and sandy soils. Low salinity is attributed to coarse soil texture with good drainage and higher relative elevation compared to surrounding lands, which reduces water retention. According to Table (4) and Figure (2), this class covers 56.29 km², representing 8.10% of the total area of Lailan.

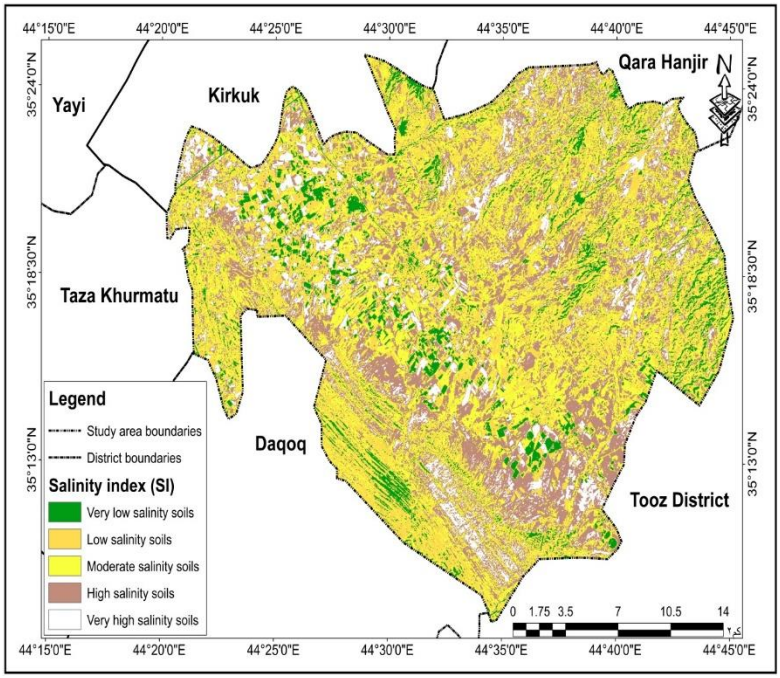


**Map 5.** Soil salinity patterns according to the SI index in Lailan Subdistrict for the year 2024.

Source: Prepared by the researcher based on the Soil Salinity Index (SI) from Landsat 8 OLI satellite imagery, dated 25/09/2024, using ArcGIS 10.4.1.

**Table 4.** Salinity levels (SI), areas (km²), and percentages (%) for Lailan Subdistrict.

| Percentage (%) | Area (km²) | Salinity Levels |
|---|---|---|
| 8.10 | 56.29 | low salinity soils Very |
| 24.60 | 170.91 | Low salinity soils |
| 31.20 | 216.8 | Moderate salinity soils |
| 27.45 | 190.71 | High salinity soils |
| 8.65 | 60.13 | Very high salinity soils |
| 100% | 694.84 | Total |

Source: Prepared by the researcher based on Map (4).

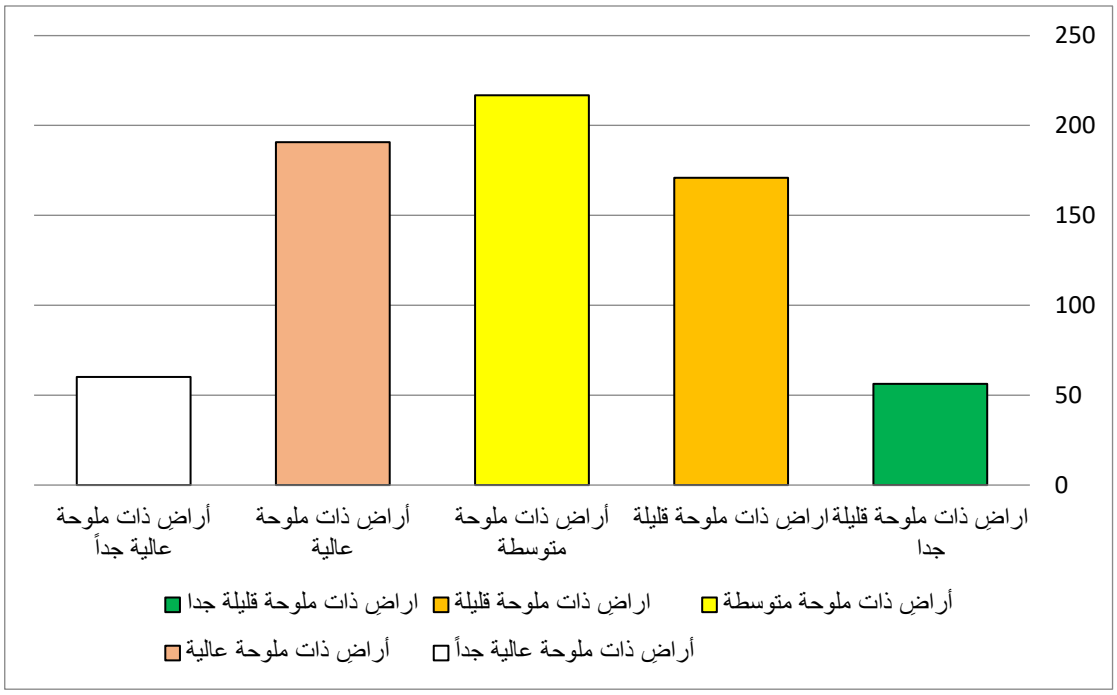


**Figure 4.** Salinity levels (SI), areas (km²), and percentages (%) for Lailan Subdistrict.
Source: Prepared by the researcher based on the data from Table (4).

**Table 5.** Classification according to soil salinity levels based on electrical conductivity (dS/m) of the surface soil paste.

| Soil Class | Soil Salinity (E.C) (dS/m) |
|---|---|
| Very Low Salinity | 4Less than |
| Low Salinity | 8 – 4 |
| Moderate Salinity | 15 – 8 |
| High Salinity | 15 –30 |
| Very High Salinity | More than 30 |

FAO UNESCO Irrigation Drainage , Salinity , An international source , Book London Hutchin son , aeko , 1973 , p. 75 .

Low Salinity Lands: Salinity ranges between 4–8 dS/m. These soils are found in some riverbanks, sandy dunes, and clay-filled basins, and are characterized by good

drainage. Their area is approximately 170.91 km², representing 24.60% of the total area of Lailan Subdistrict.

Moderately Saline Lands: Salinity ranges between 8–15 dS/m. These soils are spread across some riverbanks and poor-quality clay-filled basins, with moderate drainage. Continuous agricultural use gradually increases their salinity. Their area is about 216.8 km², accounting for 31.20%.

Highly Saline Lands: Salinity ranges between 15–30 dS/m. These lands occur in poor basins and clay-filled marshlands, where poor drainage, shallow saline groundwater, and high evaporation contribute to salt accumulation. Their area is approximately 190.71 km², representing 27.45%.

Very Highly Saline Lands: Salinity exceeds 30 dS/m. These lands are found in some irrigation channels and clay-filled marshes that have been drained and transformed into salt flats. Their area is about 60.13 km², representing 8.65%.

It is evident that the lands of Lailan Subdistrict are affected by salinization to varying degrees, mainly due to continuous agricultural use, uncontrolled irrigation, excessive irrigation relative to crop needs, high temperatures, and intense evaporation. Draining marshlands has expanded saline land areas, while some lands with low to moderate salinity have increased due to agricultural reclamation projects aimed at boosting local production.

**Desertification Risk Index (DRI):**

The Desertification Risk Index (DRI) is a key analytical tool designed to estimate the susceptibility of lands to desertification. It integrates both natural and human factors to provide a comprehensive view of the environmental condition. DRI does not only measure current desertification but also indicates the potential for future land degradation under prevailing climatic conditions and human activities.

The index analyzes key elements such as climate (rainfall amount and distribution, temperatures, drought index), soil properties (salinity, fertility, erosion susceptibility), water resources (groundwater depth, irrigation and drainage efficiency), vegetation cover (density and diversity), and human activities (overgrazing, agricultural and urban expansion, unsustainable resource use). Relative weights are assigned to these factors according to their importance and then combined mathematically to produce a composite value representing the level of risk.

Results are classified from low-risk areas, which are environmentally stable, to high-to-very-high-risk areas, which exhibit clear signs of degradation and require urgent intervention. Thus, DRI serves as an effective decision-making tool for land management, agricultural planning, and desertification mitigation strategies, commonly implemented within Geographic Information Systems (GIS) to map spatial distribution of land susceptibility.

The index is applied using the following equation:

Desertification Risk Index (DRI) = 0.10ST + 0.12SM + 0.18NDVI + 0.18SPI + 0.06ER + 0.10LU + 0.08GW + 0.18SI

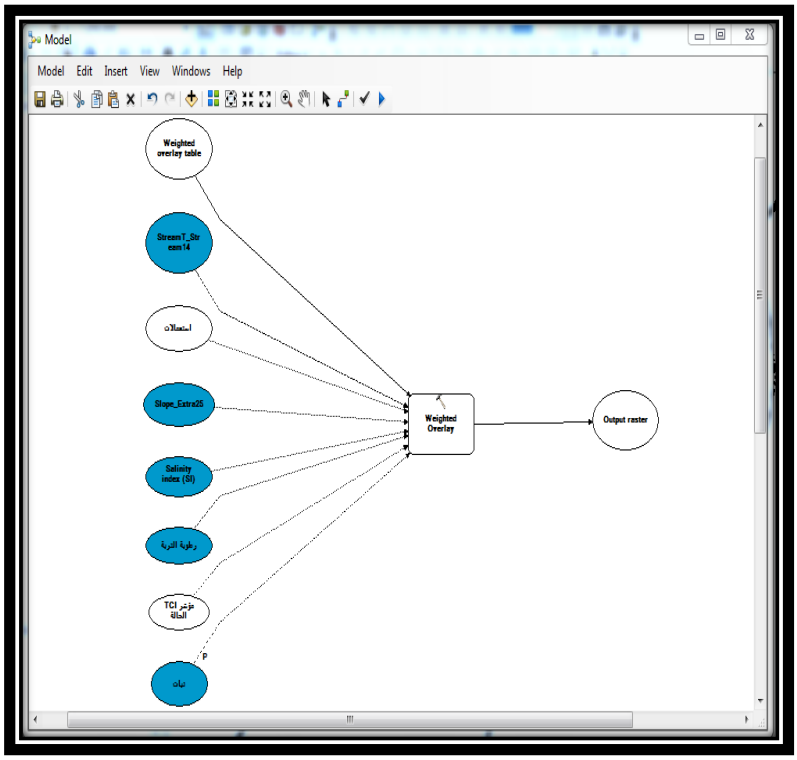


**Figure 4.** Model framework for layers of the Desertification Risk Index (DRI).
**Source: Prepared by the researcher using ArcGIS 10.4.1.**

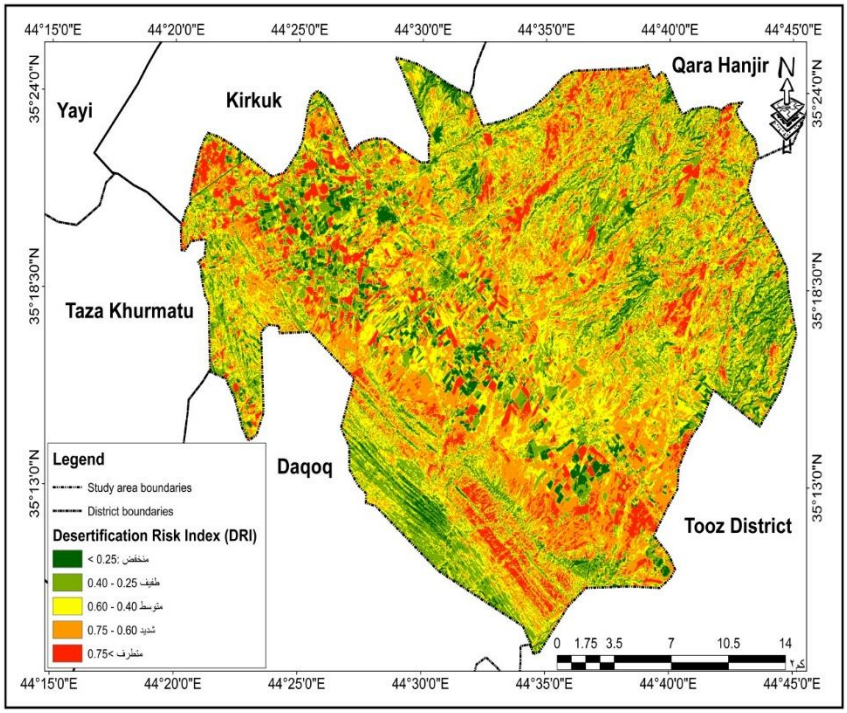


**Map 6.** Desertification Risk Index (DRI) for the study area.
Source: Prepared by the researcher based on Maps (2), (3), (4), and (5), using ArcGIS 10.4.1.

**Table 6. Desertification Risk Index (DRI) for the study area.**

| Percentage (%) | Area (km²) | Level | Class |
|---|---|---|---|
| 6.51 | 45.25 | <0.25 | Low |
| 23.82 | 165.53 | 0.40 - 0.25 | Slight |
| 30.27 | 210.35 | 0.60 - 0.40 | Moderate |
| 29.25 | 203.21 | 0.75 - 0.60 | Severe |
| 10.15 | 70.5 | 0.75 < | Extreme |
| 100% | 694.84 | Total | |

Kosmas, C., Kirkby, M., & Geeson, N. (Eds.). (1999). The MEDALUS project: Mediterranean desertification and land use. Manual on key indicators of desertification and mapping environmentally sensitive areas to desertification. European Commission, DGXII, Science, Research and Development, EUR .18882.

***Discussion***

The results of applying the Desertification Risk Index (DRI) in Lailan Subdistrict indicate a clear variation in the severity of desertification across the studied areas. The total area is 694.84 km², distributed into five main classes. The low-risk class (<0.25) occupies the smallest area, 45.25 km², representing 6.51% of the total area, reflecting the limited extent of relatively intact lands. The slight-risk class (0.25–0.40) covers 165.53 km², or 23.82%, representing areas that are still amenable to reclamation if resource management is maintained sustainably [10], [11].

The moderate-risk class (0.40–0.60) leads all classes, covering 210.35 km² (30.27%), indicating that nearly one-third of the subdistrict faces real threats, including declining soil fertility and productivity. Similarly, the severe-risk class (0.60–0.75) covers 203.21 km² (29.25%), reflecting the progression of large areas toward advanced degradation levels. The extreme-risk class (>0.75) occupies 70.5 km² (10.15%), representing lands that are nearly unsuitable for agricultural use due to soil degradation and loss of vegetation cover [12], [13].

Spatial representation of these results shows that moderate and severe desertification areas are widely distributed in the central and southeastern parts of Lailan, while extreme-risk areas are concentrated mainly in the eastern and southern regions, where drought prevails and unsustainable agricultural practices dominate. Low and slight-risk areas are limited and mainly associated with irrigated lands and intensive farming zones [14], [15].

The DRI results reveal that over 70% of Lailan Subdistrict falls within critical desertification categories (moderate, severe, extreme), highlighting the environmental and agricultural risks and emphasizing the urgent need for mitigation programs. Recommended measures include improving water resource management, implementing rainwater harvesting techniques, regulating grazing, and cultivating drought-resistant crops.

## CONCLUSION

**Fundamental Finding :** This study confirms that desertification in Lailan Subdistrict is a severe environmental challenge, with over 70% of the area falling into moderate to extreme risk classes due to combined pressures of drought, soil salinity, and unsustainable land use. **Implication :** These findings highlight the urgent need for integrated land management strategies, including efficient water resource utilization, cultivation of drought- and salt-tolerant crops, vegetation restoration, and the adoption of conservation-oriented agricultural practices to safeguard food security and sustain agricultural productivity. **Limitation :** The analysis relies primarily on remote sensing indices and GIS-based interpretation, which, while effective for large-scale monitoring, may overlook fine-scale socio-economic and soil management dynamics that influence land degradation. **Future Research :** Further studies should incorporate field-based validation, socio-economic assessments, and advanced artificial intelligence models to improve predictive accuracy, evaluate policy effectiveness, and develop adaptive frameworks that ensure resilience against desertification in both local and regional contexts.

## REFERENCES

[1] S. Sangwan, G. Saxena, and R. Prasanna, "Nature-Based Solutions for Food Security and Soil Sustainability," in *Ecological Solutions to Agricultural Land Degradation*, Springer Nature Singapore, 2025, pp. 265–281. doi: 10.1007/978-981-96-3392-0_10.

[2] P. K. Badapalli, R. B. Kottala, and P. S. Pujari, "Impact of Desertification in Semi-arid Regions," in *Aeolian Desertification*, Springer Nature Singapore, 2023, pp. 95–100. doi: 10.1007/978-981-99-6729-2_6.

[3] G. KUM, "Yarıkurak sahalarda referans evaporanstpirasyonun (Eto) alansal dağılımı ve zamansal değişimi: Şanlıurfa örneği," *Türk Coğrafya Dergisi*, no. 80, pp. 87–96, Jun. 2022, doi: 10.17211/tcd.1116059.

[4] H. Al-Jumaily and A. Alhamdany, "Geochemical distribution of Cadmium in geological formation (Miocene- Pliocene)Outcropped in Jambur area , Kirkuk Government /Northern IRAQ," *Kirkuk University Journal-Scientific Studies*, vol. 13, no. 3, pp. 337–355, Sep. 2018, doi: 10.32894/kujss.2018.13.3.23.

[5] Y. Zhang, Y. Zhang, R. Lu, S. Shu, X. Lang, and L. Yang, "Investigation of the normal spectral band emissivity characteristic within 7.5 to 13 μm for Molybdenum between 100 and 500 °C," *Infrared Physics & Technology*, vol. 88, pp. 74–80, Jan. 2018, doi: 10.1016/j.infrared.2017.11.017.

[6] W. Zhao, "Near-Infrared Radiance of Vegetation is More Sensitive Than Vegetation Indices for Monitoring NPP of Winter Wheat Under Water Stress_supp1-3402831.docx," *Institute of Electrical and Electronics Engineers (IEEE)*. doi: 10.1109/jstars.2024.3402831/mm1.

[7] X. Zheng, W. Qiao, and Z. Y. Wang, "Broad-spectrum chemiluminescence covering a 400–1400 nm spectral region and its use as a white-near infrared light source for imaging," *RSC Adv*, vol. 5, no. 122, pp. 100736–100742, 2015, doi: 10.1039/c5ra20394e.

[8] M. Zhang, D. Luo, and Y. Su, "Drought monitoring and agricultural drought loss risk assessment based on multisource information fusion," *Natural Hazards*, vol. 111, no. 1, pp. 775–801, Oct. 2021, doi: 10.1007/s11069-021-05078-w.

[9] C. Callegaro and N. Ursino, "Connectivity of Niches of Adaptation Affects Vegetation Structure and Density in Self-Organized (Dis-Connected) Vegetation Patterns," *Land Degradation & Development*, vol. 29, no. 8, pp. 2589–2594, Jun. 2018, doi: 10.1002/ldr.2759.

[10] M. Voiculescu and F. Popescu, "Management of Snow Avalanche Risk in the Ski Areas of the Southern Carpathians–Romanian Carpathians," in *Sustainable Development in Mountain Regions*, Springer International Publishing, 2016, pp. 191–213. doi: 10.1007/978-3-319-20110-8_13.

[11] B. Gomez, "Degradation of Vegetation and Agricultural Productivity due to Natural Disasters and Land Use Strategies to Mitigate Their Impacts on Agriculture, Rangelands and Forestry," in *Natural Disasters and Extreme Events in Agriculture*, Springer-Verlag, pp. 259–276. doi: 10.1007/3-540-28307-2_15.

[12] H. J. Honglin Ji, L. Y. Lilin Yi, L. X. Lei Xue, and Weisheng Hu, and W. Hu, "Upstream dispersion management of 25 Gb/s duobinary and PAM-4 signals to support 0–40 km differential reach," *Chinese Optics Letters*, vol. 15, no. 2, pp. 22502–22506, 2017, doi: 10.3788/col201715.022502.

[13] J. Spinoni, J. Vogt, G. Naumann, H. Carrao, and P. Barbosa, "Towards identifying areas at climatological risk of desertification using the Köppen-Geiger classification and FAO aridity index: TOWARDS IDENTIFYING AREAS AT CLIMATOLOGICAL RISK OF DESERTIFICATION," *International Journal of Climatology*, vol. 35, no. 9, pp. 2210–2222, Aug. 2014, doi: 10.1002/joc.4124.

[14] M. Tudeau-Clayton, "'The King's English' 'Our English'?: Shakespeare and Linguistic Ownership," in *Shakespeare and Authority*, Palgrave Macmillan UK, 2018, pp. 113–133. doi: 10.1057/978-1-137-57853-2_5.

[15] S. A. Stearns, "Student Cheating: A Dramaturgical Analysis of Identity, Deception, and Self-deception," in *The Palgrave Handbook of Deceptive Communication*, Springer International Publishing, 2019, pp. 499–514. doi: 10.1007/978-3-319-96334-1_26.

**Manal Saahi Mohammed Darwish**
Samarra University, Iraq